Available online at www.sciencedirect.com
ScienceDirect
Journal of Membrane Science 296 (2007) 21–28
journal of MEMBRANE SCIENCE
www.elsevier.com/locate/memsci

Proton exchange membranes modified with sulfonated silica nanoparticles for direct methanol fuel cells☆

Yu-Huei Su[a,b], Ying-Ling Liu[a,c,*], Yi-Ming Sun[a,d], Juin-Yih Lai[a,c], Da-Ming Wang[a,b], Yan Gao[e], Baijun Liu[e], Michael D. Guiver[e]

[a] *R&D Center for Membrane Technology, Chung Yuan University, Chungli, Taoyuan 320, Taiwan*
[b] *Institute of Polymer Science and Engineering, National Taiwan University, Taipei 104, Taiwan*
[c] *Department of Chemical Engineering, Chung Yuan University, Chungli, Taoyuan 320, Taiwan*
[d] *Department of Chemical Engineering and Material Science, Yuan Ze University, Chungli 320, Taiwan*
[e] *Institute for Chemical Process and Environmental Technology, National Research Council, Ottawa, Ont., Canada K1A 0R6*

Received 9 November 2006; received in revised form 22 February 2007; accepted 5 March 2007
Available online 14 March 2007

Abstract

Nanocomposite proton exchange membranes were prepared from sulfonated poly(phthalazinone ether ketone) (sPPEK) and various amounts of sulfonated silica nanoparticles (silica-SO_3H). The use of silica-SO_3H compensates for the decrease in ion exchange capacity of membranes observed when non-sulfonated nano-fillers are utilized. The strong $–SO_3H/–SO_3H$ interaction between sPPEK chains and silica-SO_3H particles leads to ionic cross-linking in the membrane structure, which increases both the thermal stability and methanol resistance of the membranes. The membrane with 7.5 phr of silica-SO_3H (phr = g of silica-SO_3H/100 g of sPPEK in membranes) exhibits low methanol crossover, high bound-water content, and a proton conductivity of 3.6 fold increase to that of the pristine sPPEK membrane.
© 2007 Elsevier B.V. All rights reserved.

Keywords: Proton exchange membranes; Direct methanol fuel cell; Nanoparticles

1. Introduction

Nafion® at present is one of the most advanced commercially available membranes for direct methanol fuel cells (DMFC) [1]. However, Nafion® application in DMFC is still limited by high cost and methanol crossover. Improvements in properties of the polymer electrolyte membranes have been strongly related to the developments of high performance proton exchange membranes (PEM) for DMFC. One approach is to prepare new polyelectrolytes as Nafion® alternatives. Most PEM materials are based on non-fluorinated or partially fluorinated aromatic polymers such as sulfonated polyimides [2–6] and sulfonated poly(aryl ether)s [7–12]. However, many of the reported hydrocarbon-based PEM prepared as alternatives to Nafion® still do not possess the full range or combination of desired properties for application in DMFC. Improvements in properties such as proton conductivity in low-humidity environments, chemical and oxidative stability and stability to methanol fuel solutions are some of the issues typically being addressed.

Modification of PEMs to improve their thermal and chemical stability and to depress their methanol crossover is a useful approach to improve their performance. Yamaguchi et al. [13] reported pore-filling membranes that were composed of a porous substrate and a filling polyelectrolyte. These pore-filling membranes showed high mechanical strength and low methanol crossover. Lue et al. [14] reported that plasma treatment on Nafion® surface could change its surface properties substantially with a methanol permeability reduction of 74% and without altering their bulk properties. Formation of crosslinked polyelectrolytes and polyelectrolyte interpenetrating networks are also reported to enhance PEM performance for use in DMFC [15,16]. Organic–inorganic nanocomposites represent another useful approach to PEM modification [17–21]. Layered clays and silica nanoparticles are two major inorganic reinforcements

☆ NRCC Publication 49114.

* Corresponding author at: Department of Chemical Engineering, Chung Yuan University, Chungli, Taoyuan 320, Taiwan. Tel.: +886 3 2654130; fax: +886 3 2654199.
E-mail address: ylliu@cycu.edu.tw (Y.-L. Liu).

0376-7388/$ – see front matter © 2007 Elsevier B.V. All rights reserved.
doi:10.1016/j.memsci.2007.03.007

in PEM modifications. Clay incorporation into PEMs introduces a winding pathway for a methanol molecule that results in a reduction in methanol crossover. The presence of silica nanoparticles in PEMs help to maintain water content of polymers and improves their thermal stability. The methanol crossover of the polyelectrolyte-silica nanocomposites is also reduced with the depression of their swelling degree in methanol fuel solutions.

Incorporation of nanosized inorganic reinforcements to PEMs, although bringing about membrane stabilization, would certainly lower their ion exchange capacity. To overcome this problem, Rhee et al. [22] modified Nafion® with sulfonated montmorillonite. The prepared composite membranes showed dramatic decreases in methanol permeability and high proton conductivity comparing to pristine Nafion® membranes. Bébin et al. [23] also used sulfonated Laponite particles to prepare Nafion®/clay-SO_3H composite membranes. The membrane-electrolyte assembly (MEA) based on the above mentioned membranes exhibited improved performances over Nafion® membrane-based MEA. These papers demonstrated that use of sulfonated inorganic fillers in polyelectrolyte nanocomposite membranes is an effective approach to improve the proton exchange membrane performances. Instead of clay, in this work sulfonated silica nanoparticles (silica-SO_3H) were utilized in the preparation of polyelectrolyte/silica nanocomposite membranes. Sulfonated poly(phthalazinone ether ketone) (sPPEK) with a high content of sulfonic acid groups is utilized as the proton conducting material [24]. The properties of the prepared nanocomposite PEMs are examined and discussed. A significant improvement in the membrane performance is observed with the sPPEK/silica-SO_3H nanocomposite PEMs.

2. Experimental

2.1. Materials

Sulfonated poly(phthalazinone ether ketone) with a degree of sulfonation of 1.21 (equivalent weight of sulfonated group = 514 g/mol) was obtained from direct sulfonation on poly(phthalazinone ether ketone) [24]. Silica nanoparticles with a size of 10–20 nm were purchased from Nissan Chemical Company. Sulfonation on silica nanoparticles was performed using the reported method [25,26]. From elemental analysis, the sulfur content of silica-SO_3H was 1.82 wt%, which corresponded to an equivalent concentration, 568.7 mmol/kg of –SO_3H group to silica-SO_3H.

2.2. Preparation of sPPEK/silica-SO_3H nanocomposite membranes

sPPEK (1 g, Fig. 1) was dissolved in 12 mL of *N*,*N*-dimethylacetamide (DMAc) and filtered. A measured amount of silica-SO_3H (5–30 phr, phr = g of silica-SO_3H/100 g of sPPEK in membranes) was added into the solution and stirred for 1 day to result in a homogeneous solution. The solution was then poured onto a glass plate and dried at 40 °C for 2 days. The residual solvent was evaporated at 80 °C for another 2 days. The membrane was removed from the glass plate by soaking it in water. A tough, flexible, yellowish transparent membrane was obtained after air-drying at ambient temperature.

2.3. Measurements and properties evaluation

2.3.1. Instrumental analysis

Thermogravimetric analysis was conducted with a Perkin-Elmer TGA-7. Polymer samples for TGA were preheated to 150 °C at 10 °C/min under a nitrogen atmosphere, held isothermally for 60 min, equilibrated at 80 °C, and then heated to 800 °C at 10 °C/min according to a procedure reported previously. Scanning electron micrographs were observed with a Hitachi S-3000N Hi-SEM. Energy dispersive X-ray (EDX) measurements were conducted with a Horiba ES-320 Energy Dispersive X-Ray Micro Analyzer. Water contact angles were measured with an angle-meter (Automatic Contact Angle Meter, Model CA-VP, Kyowa Interface Science Co., Ltd. Japan) at room temperature. Distilled water (5 μL) was dropped on the sample surface at ten different sites. The average of ten measured values for a sample was taken as its water contact angle. The fractions of free water in membranes were measured with a differential scanning calorimeter (Perkin-Elmer DSC 7) at a heating rate of 5 °C/min and with a nitrogen flow rate of 100 mL/min.

2.3.2. Water and methanol uptake

The membrane samples were vacuum-dried at 120 °C before testing. The sample films were soaked in de-ionized water until swelling equilibrium was attained at predetermined temperatures. The dry weight and the equilibrated swollen weight of the membranes were determined. Swollen membranes were blotted dry with tissue paper before weight measurements. The apparent water or methanol uptakes of the membranes were determined

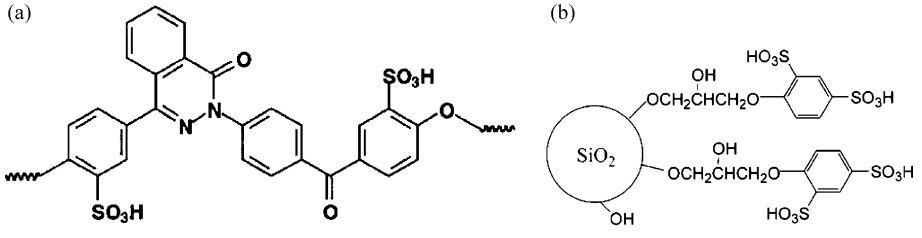

sPPEK ***silica-SO_3H***

Fig. 1. Chemical structures of polyelectrolyte sPPEK and sulfonated silica nanoparticles silica-SO_3H used in this work.

as follows:

$$\text{Uptake content}\,(\%) = \frac{W_s - W_d}{W_d} \times 100\% \quad (1)$$

where W_s and W_d are the weights of swollen and dried samples, respectively. Moreover, the apparent uptake contents from above were normalized by the sPPEK contents of the membranes to estimate the true uptake content of sPPEK polymer in the nanocomposite membranes.

2.3.3. Methanol permeation measurement by pervaporation process

The experiment was carried out according to the reported process [27]. The feed solution was in direct contact with membrane, in the pervaporation apparatus. The effective membrane area was 6.7 cm^2 and the experiments were conducted at a 50 °C feed solution. The permeation rate was determined by measuring the weight of permeate. The compositions of feed solution and permeate were analyzed by a gas chromatography (GC China Chromatography 8700 T). The separation factor of water/alcohol ($\alpha_{w/A}$) was calculated from:

$$\alpha_{w/A} = \frac{Y_W / Y_A}{X_W / X_A}$$

where X_W, X_A, Y_W, Y_A are the weight fraction of water and alcohol in the feed and permeate, respectively.

2.3.4. Proton conductivity

The proton conductivity was measured by alternating-current (ac) impedance spectroscopy over a frequency range of 1–10^7 Hz with an oscillating voltage of 50–500 mV with a system based on a Solartron 1280 gain phase analyzer. The relative humidity of proton conductivity measurement is 98%. A sample with a diameter of 3.5 mm was placed in an open, temperature-controlled cell, in which it was clamped between two blocking stainless steel electrodes with a permanent pressure of about 3 kg/cm^2. Specimens were soaked in de-ionized water before the test. The conductivity (σ) of the samples in the transverse direction was calculated from the impedance data, with the relation $\sigma = d/RS$, where d and S are the thickness and face area of the sample, respectively, and R was derived from the low intersection of the high frequency semicircle on a complex impedance plane with the Re (Z) axis.

3. Results and discussion

3.1. Preparation of sPPEK/silica-SO_3H nanocomposite membranes

The chemical structures of sPPEK polyelectrolyte and silica-SO_3H nanoparticles are shown in Fig. 1. Mixing of these two substances in DMAc formed homogeneous and transparent solutions. sPPEK/silica-SO_3H nanocomposite membranes possessing various silica-SO_3H contents (NM-SA-X, X = silica-SO_3H (g)/100 g of sPPEK in the nanocomposite membrane NM) were prepared from solution casting on glass plates. All obtained membranes showed high transparency, indicating the silica particles did not aggregate during membrane preparation. The homogeneity of dispersions of silica-SO_3H in the NM-SA nanocomposite membranes was examined with an SEM. As shown in Fig. 2a, NM-SA-5 membrane showed a very homogeneous and dense surface. No silica agglomeration occurred on the membrane surface. On the other hand, nanocomposite membrane (NM-silica-5) prepared from sPPEK and pristine silica nanoparticles (without surface sulfonation modification) [21] exhibited a micro-phase separation on the membrane surface (Fig. 2b). Silica aggregation with a domain size of about 1–2 μm appeared at the NM-silica-5 membrane surface. A possible explanation for this is that the unmodified silica nanoparticles in NM-silica-5 membrane might move toward the membrane surface during membrane preparation, due to the relatively low surface energy of silica. However, this migration of nanoparticles was not evident for silica-SO_3H in the NM-SA-5 membrane. Silica aggregation was also observed for the cross-section SEM micrograph of NM-silica-5 membrane (Fig. 2c), however, not for that of NM-SA-5 membrane (Fig. 2d). In addition, silica aggregation in NM-silica-5 membrane toward appeared at the membrane top-surface, giving further evidence to the silica migration hypothesis. Surface elemental analysis on nanocomposite membranes with an SEM-EDX provided additional information to the silica migration. As shown in Table 1, no silicon signal was detected for pristine sPPEK membrane. With the addition of 5 phr un-modified silica nanoparticles to sPPEK, the resulting NM-silica-5 membrane exhibited a silicon content of 5.4% by SEM-EDX analysis. On the other hand, only about 0.8% silicon was detected on NM-SA-5 membrane surface, indicating no silicon migration occurrence in NM-SA-5 membrane. This is in agreement to what was observed with SEM micrographs. Un-modified silica nanoparticles moved toward the membrane surface during membrane preparation, while sulfonated silica nanoparticles did not.

The sulfonic acid groups on silica surfaces restrict their motion in the sPPEK matrix. The restriction might be due to the hydrogen bonding between the sulfonic acid groups of silica-SO_3H and of sPPEK; interactions that would not exist in NM-silica-5 membrane. The –SO_3H/–SO_3H interaction might result in association of the silica-SO_3H particles, which should have ionic interaction with and be surrounded with sPPEK polymer chains, as shown in Fig. 3. The sPPEK chains also serve as separators to prevent silica-SO_3H particle aggregation. The above rationale could explain the homogeneous dispersion of silica-SO_3H particles in nanocomposite membranes, as observed by TEM (Fig. 4).

Table 1
SEM–EDX surface elemental analysis results of nanocomposite membranes

Membrane	C content (at.%)	O content (at.%)	Si content (at.%)
sPPEK	72.5	20.9	0.0
NM-silica-5	65.0	22.2	5.4
NM-SA-5	69.4	23.7	0.8
NM-SA-10	65.7	21.6	2.8
NM-SA-20	63.5	24.2	3.1

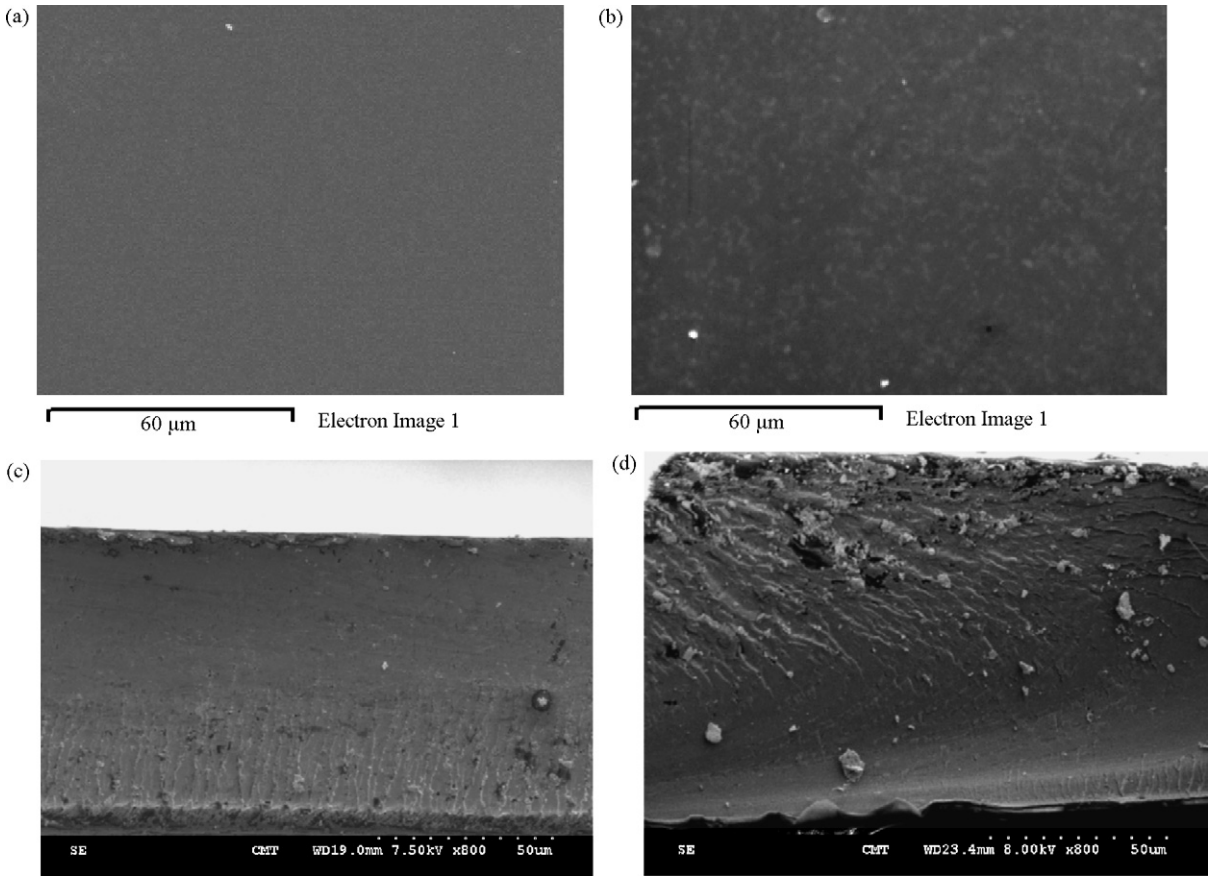

Fig. 2. SEM micrographs on nanocomposite membranes. (a) Top-surface of NM-SA-5 membrane, (b) top-surface of NM-silica-5 membrane, (c) cross-section of NM-SA-5 membrane, and (d) cross-section of NM-silica-5 membrane.

3.2. Thermal stability of sPPEK/silica-SO_3H nanocomposite membranes

The thermal stability of the sPPEK/silica-SO_3H nanocomposite membranes is of interest and was examined by TGA. Fig. 5 shows the TGA thermograms of the membranes. Pristine sPPEK and NM-silica-5 membranes exhibited similar degradation patterns (Fig. 5a). The presence of silica nanoparticles might not significantly alter the degradation behavior of sPPEK polymer [28]. However, alteration of the thermal degradation

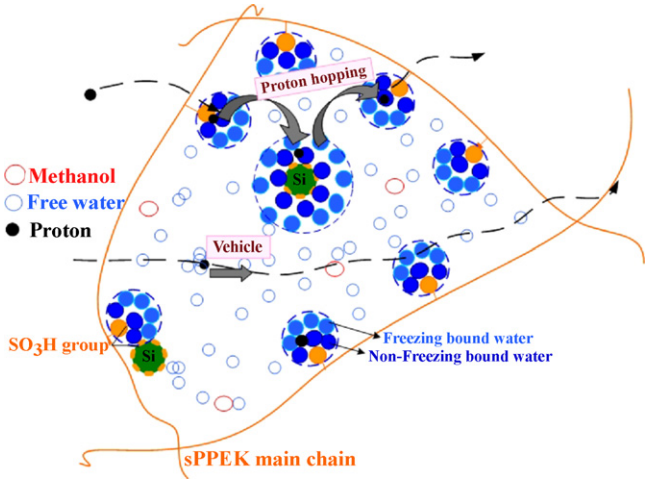

Fig. 3. Illustration on the state of water in the membranes, the interaction between the sulfonic acid groups of silica-SO_3H and of sPPEK to restrict the silica motion, and the proton-transport mechanism in the membranes.

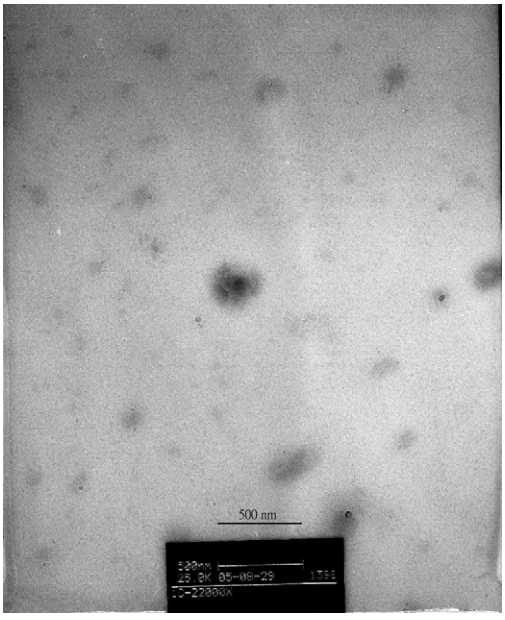

Fig. 4. TEM micrograph (×22,000) on NM-SA-5 nanocomposite membrane.

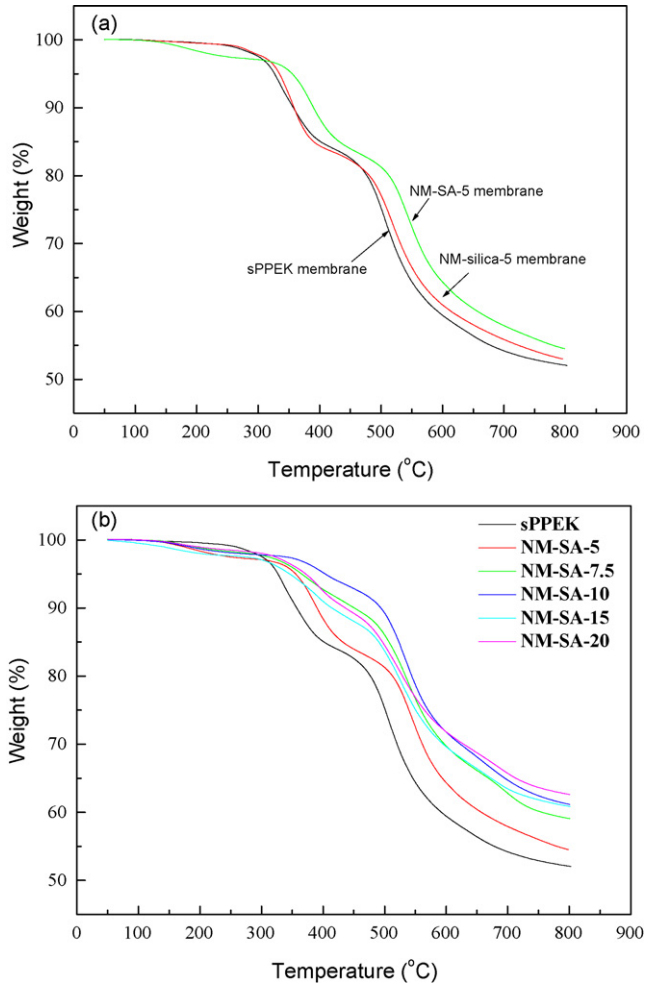

Fig. 5. TGA thermograms of sPPEK based membranes in nitrogen at a heating rate of 10 °C/min. (a) TGA thermograms of sPPEK, NM-silica-5, and NM-SA-5 membranes; (b) TGA thermograms of NM-SA nanocomposite membranes with various amounts of silica-SO_3H.

behaviors was observed with NM-SA membranes. The initial weight loss at around 150 °C was from the loss of the absorbed bound water within the membranes. However, this weight loss should not be attributed to the "poor" thermal stability of the membranes. On the other hand, the weight loss starting at about 290 °C was due to the decomposition of sulfonic acid groups [29,30], and then followed the weight loss from the polymer chain thermal degradation at about 490 °C. These two weight loss temperatures shifted toward high temperatures with addition of sulfonated silica particles. A relatively high degradation temperature and high char yield were observed with NM-SA-5 membrane. The thermal stability enhancement was more significant for membranes possessing silica-SO_3H contents above 7.5 phr (Fig. 4b). The thermal stability of these membranes was superior to pristine sPPEK. Since NM-silica-30 membrane (nanocomposite membrane containing 30 phr unmodified silica) was reported to exhibit a thermal degradation pattern similar to that of sPPEK membranes [21], the thermal stability enhancements with NM-SA membranes should not be due to the addition of silica particles, but could be attributed to the presence of sulfonic acid groups of silica particles. The presence of –SO_3H/–SO_3H interaction between functionalized silica particles and sPPEK chains formed ionic cross-linking structures so as to increase the thermal stability of the NM-SA membranes as observed in their TGA thermograms. Moreover, NM-SA-10 and NM-SA-7.5 membranes showed relatively good thermal stability among the nanocomposite membranes, indicating too many silica-SO_3H particles in the membranes might form silica-associated domains so as to lose their effect on polymer chain stabilization.

3.3. Water and methanol fuel uptakes and permeation properties

The strong interaction between silica-SO_3H and sPPEK might result in an ionic cross-linking structure to the nanocomposite membranes, which was observed with the alteration of solubility behavior of the membranes. Pristine sPPEK membrane was readily dissolved in DMAc. However, NM-SA nanocomposite membranes lost their solubility in DMAc at room temperature. NM-SA membranes were soluble in hot DMAc, due to the hydrogen-bonding interaction breaking at elevated temperatures. Formation of a cross-linking structure in NM-SA nanocomposite membrane enhances the membrane stability in solvents. Fig. 6 shows the water and methanol absorption properties of nanocomposite membranes. All nanocomposite membranes exhibited depressed water and methanol absorptions. The amounts of water and methanol absorptions leveled off for membranes possessing silica-SO_3H contents above 10 phr. Some water-absorption sites of sPPEK in NM-SA membrane were blocked with silica-SO_3H. This blocking effect could also be attributed to the presence of silica-SO_3H/sPPEK interaction, which reduces the swelling ability of sPPEK in water. Fig. 7 shows the surface water contact angles of the nanocomposite membranes. Addition of silica-SO_3H to sPPEK membranes slightly increased their membrane surface water contact angles, indicating the hydrophilic sulfonic acid groups might reverse toward membrane interior. As silica-SO_3H did not migrate to the membrane surface, the inversion of sulfonic acid groups might be induced by the –SO_3H/–SO_3H interaction. The –SO_3H groups of silica particles, which are present in the membrane

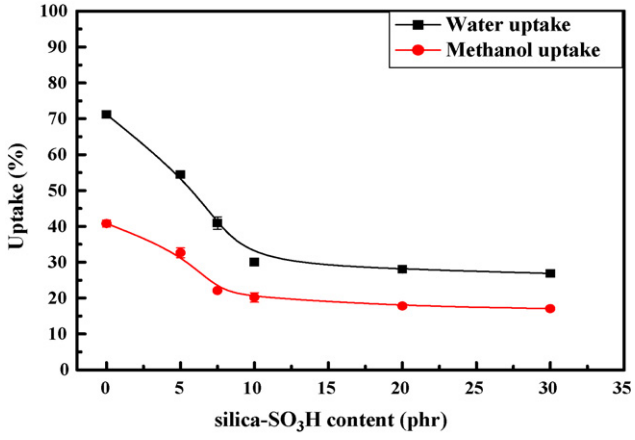

Fig. 6. Water and methanol uptakes measured on NM-SA nanocomposite membranes.

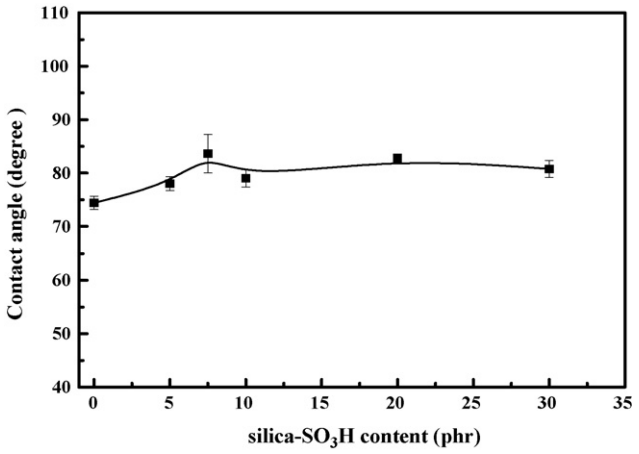

Fig. 7. Surface water contact angles of NM-SA nanocomposite membranes.

interior, attracted the $–SO_3H$ groups of sPPEK to reverse the $–SO_3H$ groups to the membrane interior. The relatively high contact angle observed with NM-SA-7.5 also implied a relatively strong $–SO_3H/–SO_3H$ interaction, as observed with thermal stability tests.

The methanol uptake values of the nanocomposite membranes were lower than their water uptakes, as shown in Fig. 6. The low methanol uptake values of NM-SA membranes implied their low affinity to methanol and low methanol crossover. The methanol permeability of the nanocomposite membranes was measured with a pervaporation test, and the results are shown in Fig. 8. With a 3 M methanol feed solution, the pristine sPPEK membrane exhibited a high flux through the membrane of about 7600 g/m^2 h. Formation of nanocomposite membranes with silica-SO_3H significantly decreased the fluxes of membranes. Methanol molecules permeate through the membranes via a two-step mechanism, i.e. dissolving into the membrane and then diffusing through the membrane (solution-diffusion mechanism). As mentioned above, NM-SA membranes exhibited relatively low affinity to methanol molecules so as to depress dissolution of methanol into the membranes. Moreover, the strong $–SO_3H/–SO_3H$ interactions between sPPEK and silica-SO_3H suppress polyelectrolyte chain motions so as to depress the methanol diffusion rate in the membranes. These two behaviors contributed to the low methanol concentration in permeates observed with the NM-SA nanocomposite membranes. In addition, the methanol concentrations at the permeate side observed for all the membranes are lower than the feed methanol concentration, indicating the membranes are resistant to methanol permeation. The lowest methanol concentration in the permeate among the tested membranes is observed with NM-SA-7.5. This result suggested that NM-SA-7.5 might possess a relatively compact and dense structure, which is more hindered for methanol molecule permeation.

In addition to the total water uptakes, the states of water molecules associated with the hydrophilic sPPEK polymer and silica-SO_3H particles are also of interest. In the reported literature [31–34] the water absorbed in the membrane can be divided broadly into two groups of bound water and free water. The bound water is the state of water associated with the membrane matrix and the free water is not. These two states of water exhibit different calorimetric behaviors and can be detected with DSC measurements [35,36]. After cooling the membrane to below 0 °C, free water will freeze whereas bound water is non-freezing. Therefore, for a heating scan on the frozen membrane sample, the heat required to melt the frozen free water can be calculated. The amount of free water in the membrane is obtained by comparing the melting enthalpy of free water to the heat of fusion of pure water (334 J/g) [32]. The amount of bound water is then obtained from the difference between the total water uptakes and the free water calculated from DSC analysis. Fig. 9 shows the contents of water in different states in the NM-SDA membranes. NM-silica-5 and NM-SA-5 membranes possessed similar free water. However, the amount of bound water in NM-SA-5 membrane was much higher than that in NM-silica-5 membrane, also indicating that addition of sulfonated silica, rather than un-modified silica, to sPPEK membranes enhanced their ability of formation hydrogen-bonding with water molecules. On the other hand, the total water, free water, and bound water contents in the membranes decreased with the addition of silica-SO_3H, indicating that the formation of nanocomposite might lead to more compact membranes. The critical amount of silica-SO_3H

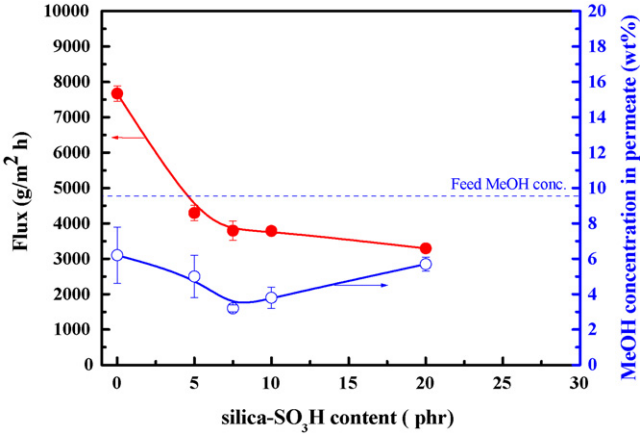

Fig. 8. Methanol permeability of NM-SA nanocomposite membranes.

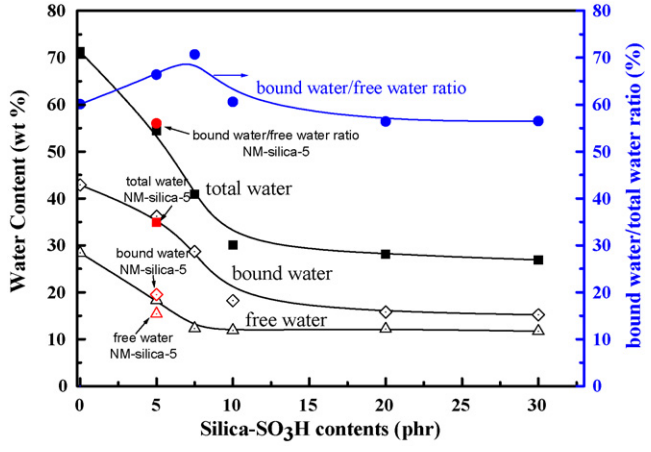

Fig. 9. The change of water uptakes in the NM-SA nanocomposite membranes as a function of the amounts of silica-SO_3H.

in membranes for depression of total water and bound water is about 10 phr. On the other hand, the critical value for free water is about 7.5 phr. Since the free water is present in the membrane space between the sulfonic acid groups, this result indicates that the silica-SO_3H amount of 7.5 phr is enough to lead an ionic cross-linking of the membrane with reduced spaces between polymer chains and silica particles. This result is also coincident to that observed with methanol permeation analysis. Moreover, the NM-SA-7.5 membrane exhibited the highest bound water fraction (the bound water amount over the total water amount). Holdcroft and co-workers [37] reported that proton conductivity in membranes may be achieved via strongly bound water. The ability of bound water to facilitate the transport of protons originates by generation of a continuous proton conductive pathway. Therefore, NM-SA-7.5 membrane might exhibit a relatively high proton conductivity among the prepared membranes, which is discussed below.

3.4. Proton conductivity

The proton conductivity of the nanocomposite membranes measured at different temperatures is shown in Fig. 10. Addition of un-modified silica to sPPEK (NM-silica-5) caused a reduction in sulfonic acid group concentration so as to lower the membrane's proton conductivity. This proton conductivity reduction can be compensated with using sulfonated silica-SO_3H. NM-SA-5 membrane exhibited higher proton conductivities than NM-silica-5 membrane. It is also noteworthy that the proton conductivities measured with NM-SA-5 membranes at elevated temperatures are higher than those measured with sPPEK membrane. It is demonstrated that addition of the sulfonated silica nanoparticles to sPPEK can further enhance its proton conductivity with introduction of additional sulfonic acid groups. NM-SA-7.5 showed the highest proton conductivities among the nanocomposite membranes. The proton conductivity of the NM-SA-7.5 PEM is about 3.6-fold to that of the unmodified sPPEK membrane. Generally, two principle mechanisms of vehicle mechanism and Grotthus mechanism (hopping) describe proton diffusion through the membrane [38]. It is possible that the bound water participates by the Grotthus mechanism, and the free water takes part mostly by vehicle mechanism [39]. Addition of silica-SO_3H to the membranes increases the bound water contents in the membranes (Fig. 3). The bound water facilitates the proton transport ability through the Grotthus mechanism, originating by generation of a continuous proton conductive pathway. Therefore, the high proton conductivity of NM-SA-7.5 can be attributed to the high bound water contents in the membrane.

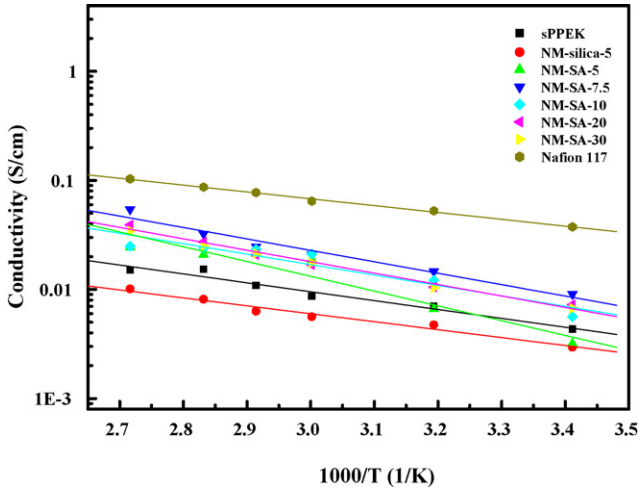

Fig. 10. The proton conductivities of nanocomposite membranes at various temperatures.

4. Conclusions

The incorporation of sulfonated silica nanoparticles into sulfonated polymers to form nanocomposite membranes simultaneously improves their thermal stability and reduces methanol crossover. The ionic interactions between the sulfonated silica nanoparticles and the sulfonated polymer play an important part in the improvement of properties. With a high fraction of bound water in the nanocomposite membrane, the membrane comprising 7.5 phr of sulfonated silica nanoparticles might yield a continuous proton conductive pathway to ensure its high proton conductivity, with a value of about 3.6-fold to that of the pristine sPPEK membrane.

Acknowledgements

This work is supported by the joint research cooperation program between the National Science Council Taiwan (Grant No. NSC 95-2218-E-033-007) and the National Research Council of Canada. Partial financial support for this work from the Taiwan Power Company is also highly appreciated.

References

[1] D.E. Curtin, R.D. Lousenburg, T.J. Henry, P.C. Tangeman, M.E. Tisack, Advanced materials for improved PEMFC performance and life, J. Power Sources 131 (2004) 41–48.
[2] K. Miyatake, N. Asano, M. Watanabe, Synthesis and properties of novel sulfonated polyimides containing 1,5-naphthylene moieties, J. Polym. Sci. Part A: Polym. Chem. 41 (2003) 3901–3907.
[3] W. Jang, S. Sundar, S. Choi, Y.G. Shul, H. Han, Acid-base polyimide blends for the application as electrolyte membranes for fuel cells, J. Membr. Sci. 280 (2006) 321–329.
[4] G. Meyer, G. Gebel, L. Gonon, P. Capron, D. Marscaq, C. Marestin, R. Mercier, Degradation of sulfonated polyimide membranes in fuel cell conditions, J. Power Sources 157 (2006) 293–301.
[5] X.H. Ye, H. Bai, W.S.W. Ho, Synthesis and characterization of new sulfonated polyimides as proton-exchange membranes for fuel cells, J. Membr. Sci. 279 (2006) 570–577.
[6] Y. Yin, O. Yamada, S. Hayashi, K. Tanaka, H. Kita, K.I. Okamoto, Chemically modified proton-conducting membranes based on sulfonated polyimides: Improved water stability and fuel-cell performance, J. Polym. Sci. Part A: Polym. Chem. 44 (2006) 3751–3762.
[7] S. Gu, G.H. He, X.M. Wu, C.N. Li, H.J. Liu, C. Lin, X.C. Li, Synthesis and characteristics of sulfonated poly(phthalazinone ether sulfone ketone) (SPPESK) for direct methanol fuel cell (DMFC), J. Membr. Sci. 281 (2006) 121–129.
[8] C.G. Cho, Y.S. Kim, X. Yu, M. Hill, J.E. McGrath, Synthesis and characterization of poly(arylene ether sulfone) copolymers with sulfonimide side

groups for a proton-exchange membrane, J. Polym. Sci. Part A: Polym. Chem. 44 (2006) 6007–6014.
[9] B.J. Liu, G.P. Robertson, M.D. Guiver, Y.M. Sun, Y.L. Liu, J.Y. Lai, S. Mikhailenko, S. Kaliaguine, Poly(aryl ether ether ketone ketone)s containing fluorinated moieties as proton exchange membrane materials, J. Polym. Sci. Part B: Polym. Phys. 44 (2006) 2299–2310.
[10] B.J. Liu, D.S. Kim, J. Murphy, G.P. Robertson, M.D. Guiver, S. Mikhailenko, S. Kaliaguine, Y.M. Sun, Y.L. Liu, J.Y. Lai, Fluorenyl-containing sulfonated poly(aryl ether ether ketone ketone)s (SPFEEKK) for fuel cell applications, J. Membr. Sci. 280 (2006) 54–64.
[11] X. Zhang, S. Liu, L. Liu, J. Yin, Partially sulfonated poly(arylene ether sulfone)-b-polybutadiene for proton exchange membrane, Polymer 46 (2005) 1719–1723.
[12] Y. Yang, Z. Shi, S. Holdcroft, Synthesis of sulfonated polysulfone-block-PVDF copolymers: enhancement of proton conductivity in low ion exchange capacity membranes, Macromolecules 37 (2004) 1678–1681.
[13] T. Yamaguchi, F. Miyata, S. Nakao, Polymer electrolyte membranes with a pore-filling structure for a direct methanol fuel cell, Adv. Mater. 15 (2003) 1198–1201.
[14] S.J. Lue, T.S. Shih, T.C. Wei, Plasma modification on a Nafion® membrane for direct methanol fuel cell applications, Korean J. Chem. Eng. 23 (2006) 441–446.
[15] D.S. Kim, H.B. Park, J.W. Rhim, Y.M. Lee, Preparation and characterization of crosslinked PVA/SiO_2 hybrid membranes containing sulfonic acid groups for direct methanol fuel cell applications, J. Membr. Sci. 240 (2004) 37–48.
[16] J.A. Kerres, Blended and cross-linked ionomer membranes for application in membrane fuel cells, Fuel Cells 5 (2005) 230.
[17] W. Xu, T. Lu, C. Liu, W. Xing, Low methanol permeable composite Nafion®/silica/PWA membranes for low temperature direct methanol fuel cells, Electrochim. Acta 50 (2005) 3280–3285.
[18] H.Y. Chang, C.W. Lin, Proton conducting membranes based on PEGF/SiO_2 nanocomposites for direct methanol fuel cells, J. Membr. Sci. 218 (2003) 295–306.
[19] M.L. Di Vona, D. Marani, A. D'Epifanio, E. Traversa, M. Trombetta, S. Licoccia, A covalent organic/inorganic hybrid proton exchange polymeric membranes: synthesis and characterization, Polymer 46 (2005) 1754–1758.
[20] R.K. Nagarle, G.S. Gohil, V.K. Shahi, R. Rangarajan, Organic-inorganic hybrid membranes: thermally stable cation-exchange membrane prepared by the sol-gel method, Macromolecules 37 (2004) 10023–10030.
[21] Y.H. Su, Y.L. Liu, Y.M. Sun, J.Y. Lai, M.D. Guiver, Y. Gao, Using silica nanoparticles modifying sulfonated poly(phthalazinone ether ketone) membrane for direct methanol fuel cell: a significant improvement on cell performance, J. Power Sources 155 (2006) 111–117.
[22] C.H. Rhee, H.K. Kim, H. Chang, J.S. Lee, Nafion®/sulfonated montmorillonite composite: a new concept electrolyte membrane for direct methanol fuel cells, Chem. Mater. 17 (2005) 1691–1697.
[23] P. Bébin, M. Caravanier, H. Galiano, Nafion®/clay-SO_3H membrane for proton exchange membrane fuel cell application, J. Membr. Sci. 278 (2006) 35–42.
[24] Y. Gao, G.P. Robertson, M.D. Guiver, X. Jian, Synthesis and characterization of sulfonated poly(phthalazinone ether ketone) for proton exchange membrane materials, J. Polym. Sci. Part A: Polym. Chem. 41 (2003) 497–507.
[25] Y.L. Liu, C.Y. Hsu, M.L. Wang, H.S. Chen, A novel approach of chemical functionalization on nano-scaled silica particles, Nanotechnology 14 (2003) 813–819.
[26] Y.L. Liu, C.Y. Hsu, Y.H. Su, J.Y. Lai, Chitosan-silica complex membranes from sulfuric acid functionalized silica nanoparticles for pervaporation dehydration of ethanol-water solutions, Biomacromolecules 6 (2005) 368–373.
[27] K.R. Lee, Y.H. Wang, M.Y. Teng, D.J. Liaw, J.Y. Lai, Preparation of aromatic polyamide membrane for alcohol dehydration by pervaporation, Eur. Polym. J. 35 (1999) 861–866.
[28] Y.L. Liu, C.Y. Hsu, K.Y. Hsu, Poly(methylmethacrylate)-silica nanocomposite films from surface-functionalized silica nanoparticles, Polymer 46 (2005) 1851–1856.
[29] X. Ye, H. Bai, W.S.W. Ho, Synthesis and characterization of new sulfonated polyimides as proton-exchange membranes for fuel cells, J. Membr. Sci. 279 (2006) 570–577.
[30] J. Schmeisser, S. Holdcroft, J. Yu, T. Ngo, G. McLean, Photocuring and photolithography of proton-conducting polymers bearing weak and strong acids, Chem. Mater. 17 (2005) 387–394.
[31] L.E. Karisson, B. Wesslén, P. Jannasch, Water absorption and proton conductivity of sulfonated acrylamide copolymers, Electrochim. Acta 47 (2002) 3269–3275.
[32] S.P. Kusumocahyo, K. Sano, M. Sudoh, M. Kensaka, Water permselectivity in the pervaporation of acetic acid-water mixture using crosslinked poly(vinyl alcohol) membranes, Sep. Purif. Technol. 10 (2000) 141–150.
[33] J.W. Rhim, H.B. Park, C.S. Lee, J.H. Jun, D.S. Kim, Y.M. Lee, Crosslinked poly(vinyl alcohol) membranes containing sulfonic acid group: proton and methanol transport through membranes, J. Membr. Sci. 238 (2004) 143–151.
[34] D.S. Kim, H.B. Park, J.W. Rhim, Y.M. Lee, Proton conductivity and methanol transport behavior of cross-linked PVA/PAA/silica hybrid membranes, Solid State Ionics 176 (2005) 117–126.
[35] B. Gupta, O. Haas, G.G. Scherer, Proton exchange membranes by radiation grafting of styrene onto FEP films. IV. Evaluation of the states of water, J. Appl. Polym. Sci. 57 (1995) 855–862.
[36] S. Hietala, S. Holmberg, J. Nasman, D. Ostrovskii, M. Paronen, R. Serimaa, F. Sundholm, L. Torell, M. Torkkeli, The state of water in styrene-grafted and sulfonated poly(vinylidene fluoride) membranes, Angew. Macromol. Chim. 535 (1997) 151–167.
[37] A. Siu, J. Schmeisser, S. Holdcroft, Effect of water on the low temperature conductivity of polymer electrolytes, J. Phys. Chem. B 110 (2006) 6072–6080.
[38] K.D. Kreuer, Proton conductivity: materials and applications, Chem. Mater. 8 (1996) 610–641.
[39] D.S. Kim, B. Liu, M.D. Guiver, Influence of silica content in sulfonated poly(arylene ether ether ketone ketone) (SPAEEKK) hybrid membranes on properties for fuel cell application, Polymer 47 (2006) 7871–7880.